Ordering of FeCo nanocrystalline phase in FeCoNbBCu alloys

2003 J. Phys.: Condens. Matter 15 7843

(http://iopscience.iop.org/0953-8984/15/46/003)

INSTITUTE OF PHYSICS PUBLISHING JOURNAL OF PHYSICS: CONDENSED MATTER

J. Phys.: Condens. Matter **15** (2003) 7843–7849 PII: S0953-8984(03)68481-X

Ordering of FeCo nanocrystalline phase in FeCoNbBCu alloys

J S Blázquez[1], **A Conde**[1] **and J M Grenèche**[2,3]

[1] Departamento de Fisica Materia Condensada, CSIC-Universidad de Sevilla, Apartado 1065, 41080 Sevilla, Spain
[2] Laboratoire de Physique de L'Etat Condensé, UMR CNRS 6087, Université du Maine, 72085 Le Mans, France

E-mail: greneche@univ-lemans.fr

Received 4 September 2003
Published 7 November 2003
Online at stacks.iop.org/JPhysCM/15/7843

Abstract

The influence of both compositional changes and ordered/disordered structure on hyperfine parameters of the body-centred-cubic α-FeCo phase is discussed in terms of the binomial distribution and nearest-neighbour approximation. In the nanocrystalline alloy series $Fe_{78-x}Co_xNb_6B_{15}Cu_1$, it was found that, for the alloy with $x = 18$, nanocrystalline grains present a disordered structure, whereas for the alloys with 39 and 60 at.% Co, a tendency to an FeCo atomic ordering is observed.

1. Introduction

FINEMET (FeSiBNbCu) [1] and NANOPERM (FeMB or FeMBCu with M = Zr, Nb, Hf) [2, 3] nanocrystalline alloys are, at the present time, among the softest ferromagnetic materials known at room temperature [4]. Such properties are due to their characteristic microstructure, in which ferromagnetic nanosized α-Fe(Si) crystallites are embedded in a residual amorphous matrix, enriched in B and M atoms, also ferromagnetic but with a lower Curie temperature. Unfortunately, the outstanding soft magnetic properties of these materials are lost above the Curie temperature of the amorphous phase [5], restricting their applicability to temperatures below about 600 K. The development of HITPERM (FeCoMBCu) alloys [6] extends the temperature range of applicability of nanocrystalline alloys up to higher temperatures, due to the partial substitution of Co for Fe, which increases the Curie temperature of the amorphous matrix.

For FINEMET alloys, it has been shown that the crystalline phase exhibits an ordered Fe_3Si structure, which can be detected by conventional x-ray diffraction techniques [1, 7]. However, for HITPERM alloys, it is not possible to distinguish between ordered (simple cubic α'-FeCo) and disordered phase (body centred cubic α-FeCo) using conventional x-ray

[3] Author to whom any correspondence should be addressed.

diffraction techniques, due to the very similar scattering factors of Fe and Co. Therefore, not so accessible x-ray techniques might be used to detect the ordered phase: e.g. for $Fe_{44}Co_{44}Zr_7B_4Cu_1$ alloy, the ordered α'-FeCo phase was detected using synchrotron radiation and the anomalous scattering effect [6]. However, other indirect measurements can also give information about the degree of order of the crystalline phase. In fact, clear differences were observed in the magnetization of FeCo binary alloys [8] as well as in electronic properties such as optical conductivity [9]. For the present compositions, the partitioning of Fe and Co can be studied by ^{59}Co nuclear magnetic resonance [10] and ^{57}Fe Mössbauer spectrometry (MS) [11–13]. Indeed, those short-range-order-sensitive techniques do allow us to distinguish between ordered and disordered atomic structures. In the case of MS, the differences between the hyperfine parameters of the ordered and disordered structures are equivalent to those induced by a change of composition about 10 at.%, being $\sim$1 T and $\sim$0.02 mm s^{-1} for an average hyperfine field (B_{hyp}) and isomer shift (IS), respectively, for $Fe_{50}Co_{50}$ composition [11].

In a previous study, it was concluded that the nanocrystallization process of $Fe_{39}Co_{39}Nb_6B_{15}Cu_1$ alloy leads to the presence of an ordered α'-FeCo alloy crystalline grain, as pointed out by ^{57}Fe MS [14]. In this work, we propose a very simple model based on nearest-neighbour (NN) and binomial distributions to clarify the influence of the compositional changes and the degree of order on both B_{hyp} and IS obtained for the nanocrystalline phase of the alloy series $Fe_{78-x}Co_xNb_6B_{15}Cu_1$ ($x = 18, 39, 60$).

2. Experimental section

Melt-spun ribbons ($\sim$20 μm thick and 5 mm wide) with the compositions referred to above were studied after annealing under an argon atmosphere at 10 K min^{-1} (up to 873 K for those alloys with 18 and 39 at.% Co, or 823 K for the 60 at.% Co-containing alloy). At this stage, the nanocrystallization process is nearly complete and high volumetric fractions of α-FeCo nanocrystalline grains are obtained (0.50–0.55 for 18 and 39 at.% of Co and 0.40–0.45 for 60 at.% of Co) [15, 16]. The mean size of the crystalline grains was estimated at about 5 nm from transmission electron microscopy for the three nanocrystalline alloys [17]. Transmission MS was performed at room temperature, using a ^{57}Co source diffused into a Rh matrix. The values of the hyperfine parameters were refined using the MOSFIT program [18] and the values of the ISs are quoted relative to α-Fe foil at 300 K. The fitting procedure has been done using a discrete number of magnetic components for the crystalline phase, based on a neighbouring model. Indeed, both the B_{hyp} and the IS are sensitive to the atomic surroundings. Several fitting assumptions (linewidths, quadrupole shift and correlations between parameters) were made to check the validity of the resulting hyperfine data. It allows us to estimate thus the error bar for the mean values of the hyperfine field and IS at 0.3 T and 0.003 mm s^{-1}, respectively. The neighbouring model has been restricted to NN, neglecting the influence of the next-nearest-neighbours (NNN) shell. As can be seen below, the complexity of the studied system prevents us from extracting very fine information from it. Therefore, the simplest model has been chosen to describe the system in terms of the least number of factors with the maximum effect, allowing some relevant conclusions to be drawn.

3. Local order modelling

From three-dimensional atom–probe results, it was possible to infer a homogeneous Co distribution throughout the nanocrystalline grains and the residual amorphous matrix [19]. Therefore, the mean composition of the crystalline phase formed during nanocrystallization

is assumed to be $Fe_{100-x}Co_x$ (x being the Co content of the initial amorphous alloy), where both Nb and B atoms are rejected from the nanocrystalline grains into the amorphous matrix, as has been discussed elsewhere [14].

Using a binomial distribution, the probability of a BCC environment with n Fe atoms and $8 - n$ Co atoms as NN is given by the expression

$$P = M x_{\mathrm{Fe}}^{n} x_{\mathrm{Co}}^{8-n} \tag{1}$$

where x_{U} is the concentration of atoms U (Fe or Co) in the set of 8 atoms that surrounds the central Fe and M is the multiplicity, calculated as

$$M = 8!/[(8-n)!n!]. \tag{2}$$

However, the composition of the neighbourhood of the Fe atoms must be strongly affected, not only by the global composition, but also by the ordered or disordered structure of the crystalline grains. Two extreme situations have been considered: maximum ordered and fully disordered structures.

In a disordered structure, the Co and Fe positions are indistinguishable and their distribution would be random. It is important to note that, from a MS point of view, among the nine atoms which form the cluster unit, the central one is forced to be Fe. Therefore, the probabilities for finding a Co or Fe atom in the environment are modified with respect to the global composition ($x'_{\mathrm{Fe}} + x'_{\mathrm{Co}} = 1$). In fact, the average number of Fe atoms in the group of nine is $9x'_{\mathrm{Fe}}$ and the average number of Co atoms is $9x'_{\mathrm{Co}}$. Taking into account that one atom is the central probed Fe, the average number of Fe atoms in the 8 NN will be $9x'_{\mathrm{Fe}} - 1$ and thus the concentration in the NN environment is $x_{\mathrm{Fe}} = (9x'_{\mathrm{Fe}} - 1)/8$ and in the case of Co it is $x_{\mathrm{Co}} = (9x'_{\mathrm{Co}})/8$.

In an ordered α'-FeCo structure, the positions of both Co and Fe atoms in the elementary cell are distinguishable, e.g. Fe in $(0, 0, 0)$ and Co in $(1/2, 1/2, 1/2)$. For compositions different to $Fe_{50}Co_{50}$, it has been considered that the maximum ordered structure corresponds to a system in which a minority of atoms (Fe or Co) is located in their correct positions while the residual positions corresponding to this atom are occupied with the other atom with concentrations higher than 50 at.%. Therefore, the latter sort of atom would be in both correct and incorrect sites, whereas the former would occupy only correct sites.

4. Results and discussion

Once the concentration in the NN zone has been calculated, it is straightforward from (1) to calculate the probabilities of the different environments, depending on the average composition and on the ordered/disordered structure. The correspondence between the NN environment and the hyperfine field at the Fe probe has been performed using literature values corresponding to BCC FeCo binary alloys [11–13]. The proposed hypothesis is that B_{hyp} corresponding to a NN environment might be similar to the average value of B_{hyp} for a disordered α-FeCo system with the same composition as that exhibited by the explored set of nine atoms. On the other hand, with the increase in Co concentration in the α-FeCo disordered phase, IS increases from 0 to $\sim$0.04 mm s^{-1}, from 0 to 30 at.% of Co, respectively, and then decreases to $\sim$0.02 mm s^{-1} for 75 at.% of Co [11, 12]. Therefore, two linear regimes were considered in obtaining the value of IS corresponding to a given NN environment. Table 1 shows the NN environments with the corresponding B_{hyp}, IS and the calculated probabilities for disordered and ordered structures of the different compositions of the present study.

For comparison with these theoretical results, the experimental Mössbauer spectra have been fitted, assuming seven different magnetic sextets corresponding to the different values

Table 1. Hyperfine field (B_{hyp}) and IS assigned to the different NN environments, along with theoretical probabilities in the maximum ordered and fully disordered structures.

Number Co in NN	B_{hyp} (T)	IS (mm s^{-1})	60 at.% Co alloy		39 at.% Co alloy		18 at.% Co alloy	
			Disordered	Ordered	Disordered	Ordered	Disordered	Ordered
0	33.0	0	∼1E−4	0	0.010	0.180	0.164	0.407
1	35.0	0.013	0.002	0	0.062	∼1E−4	0.332	0.077
2	36.5	0.027	0.015	0	0.168	0.002	0.295	0.152
3	37.0	0.040	0.062	0	0.263	0.011	0.150	0.171
4	35.5	0.035	0.162	0	0.257	0.050	0.048	0.120
5	34.5	0.030	0.269	0	0.161	0.141	0.010	0.054
6	34.0	0.025	0.280	0	0.063	0.250	0.001	0.015
7	33.0	0.020	0.166	0	0.014	0.254	∼1E−4	0.002
8	33.0	0.015	0.043	1	0.001	0.112	∼1E−6	∼1E−4

of B_{hyp} presented in table 1. One observes that three NN configurations correspond to the lowest field, 33.0 T (0, 7 and 8 Co atoms as NN), whereas all other NN configurations have been individually associated to a discrete value of B_{hyp}. Therefore, these latter values of B_{hyp} correspond to discrete values of IS (fixed during the fitting procedure and shown in table 1), whereas for the 33.0 T contribution, IS was maintained free in the 39 and 60 at.% Co alloys. However, for 18 at.% Co alloy, it is observed that the probability of the NN configurations with seven or eight Co atoms is much lower than that corresponding to 0 Co atoms in both cases, ordered and disordered structures. Therefore, for 18 at.% Co alloy the IS value assigned to the 33.0 T contribution was fixed at 0 mm s^{-1}, corresponding to 0 Co NN atoms. The amorphous component was fixed equal to that obtained previously [14]. Therefore, only the parameters assigned to the crystalline phase were fitted. The width of the different spectral lines corresponding to the crystalline contributions was fixed to 0.22 or 0.23 mm s^{-1}, except for the contribution at 33.0 T, for which it was assumed to be equal to 0.30 mm s^{-1}. The small width of the lines thus avoids the overlapping between them and thus the emergence of oscillations [20]. In the case of the 33.0 T contribution, a wider line with a typical width of 0.30 mm s^{-1} could be used because this contribution is 1 T smaller than the second one at 34.0 T and is therefore better resolved than the others which are separated by 0.5 T between them. We have checked that the fitting procedure does not influence the average values of both B_{hyp} and IS obtained previously. They were not affected, except the $\langle IS \rangle$ value for the crystalline phase for the alloy with 18 at.% of Co, in which $\langle IS \rangle$ changes slightly from 0.040($\pm$0.005) mm s^{-1} [14] to 0.030($\pm$0.005) mm s^{-1}. This fact allows us to be more confident of the B_{hyp} values.

Figure 1 shows the Mössbauer spectra for the different samples studied along with the corresponding theoretical spectra obtained from the fitting procedure. Figure 2 exhibits the experimental field distribution along with the calculated ones for both ordered and disordered phases. The comparison might not be very restrictive, taking into account the uncertainty of the hyperfine fields assigned to the different NN environments. However, a discussion in terms of low, medium and high field contributions (33; 34.5–35.5 and 36.5–37 T, respectively) can be emphasized. In the case of experimental 18 at.% Co, it is clear that high field contributions are predominant, as is found in the disordered structure and different to the well ordered structure, in which 33 T is the highest contribution.

For 39 at.% Co alloy, although the 33 T contribution is not as high as in the maximum ordered structure, high field contributions are the lowest ones, whereas, in the disordered structure, a quite important contribution corresponds to 36.5 and 37 T. The value of IS obtained corresponding to the 33 T contribution is 0.024 $\pm$ 0.007 mm s^{-1}, which is closer

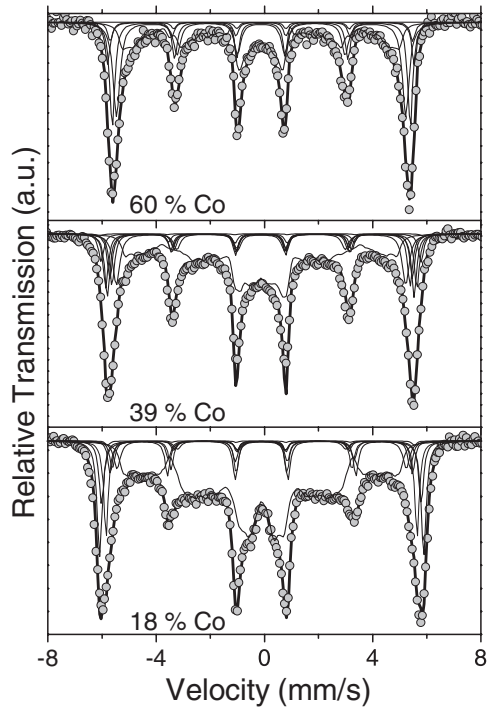

Figure 1. Experimental and corresponding theoretical MS spectra of the three alloys studied.

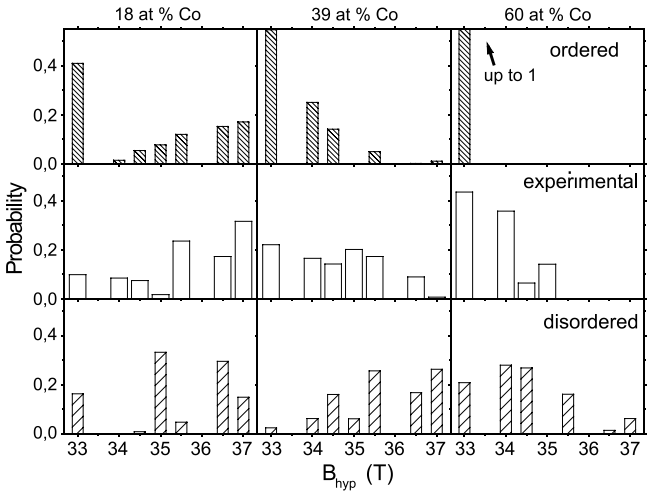

Figure 2. Distribution of probabilities of the different B_{hyp} contributions for maximum ordered and fully disordered structures, both theoretical and experimental, depending on the Co content of the crystals.

to the corresponding value for 7 Co as NN (0.020 mm s^{-1}), indicating that this is the main contribution to 33 T. However, this is in agreement with ordered and disordered structures.

Finally, for 60 at.% Co alloy, it is clear that other contributions different from 33 T appear, as occurs in the disordered structure. However, the 33 T contribution is higher than that

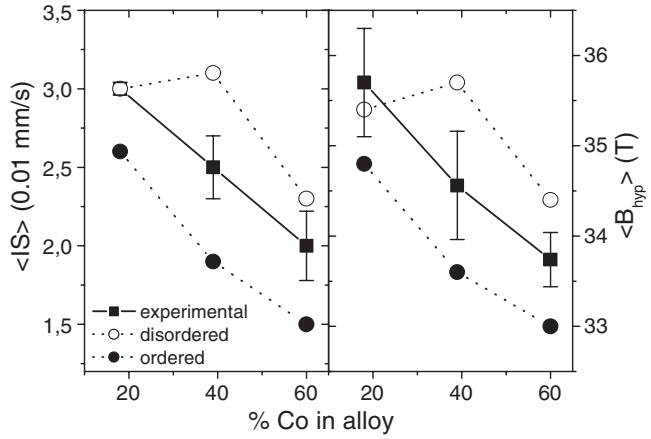

Figure 3. Average values of IS (left) and hyperfine field (right), for experimental (squares) and theoretical structures, maximum ordered (full circles) and fully disordered (hollow circles), versus Co content of the alloy. In the case of B_{hyp}, the error bars were estimated from those of the different contributions during the fitting procedure, whereas, in the case of IS, the error bar for IS for the contribution with 33 T has also been considered.

theoretically predicted in the fully disordered structure, while the high field contribution can be neglected. Moreover, the IS value for the 33 T contribution is 0.017 ± 0.004 mm s^{-1}, close to the value corresponding to 8 Co as NN (0.015 mm s^{-1}), which is the only contribution for the ordered configuration.

From this fact, it is inferred that the nanocrystalline grains of the alloys with 39 and 60 at.% of Co display a structure closer to the ordered state than that of the nanocrystals of the 18 at.% Co alloy. This is in agreement with the compositions of nanocrystalline grains, $Fe_{61}Co_{39}$ and $Fe_{40}Co_{60}$, for 39 and 60 at.% Co, respectively, for which the α'-FeCo phase is stable even at the annealing temperature (873 and 823 K, respectively) [21], whereas, for $Fe_{82}Co_{18}$, the disordered phase is the stable one. The evolution of the lattice parameter of the FeCo phase after the second transformation stage, explained in terms of an ordering tendency of the nanocrystalline grains due to the composition's proximity to $Fe_{50}Co_{50}$ [22] also agrees with the present results.

Figure 3, which compares experimental data to theoretical predictions within the accuracy limitations as previously discussed, shows that the weighted average values of both B_{hyp} and IS are rather consistent with the previous results. In addition, both plots suggest that the alloy with 18 at.% Co possesses a disordered crystalline phase, whereas for the 39 and 60 at.% Co alloy, crystals present a tendency towards the ordered structure.

5. Conclusions

^{57}Fe MS allows us to obtain information about the ordered/disordered structure of the FeCo crystalline phase in HITPERM-type alloys. In the present work devoted to the $Fe_{78-x}Co_xNb_6B_{15}Cu_1$ series, a tendency to the FeCo atomic ordered structure has been found in the crystalline phases of alloys with $x = 39$ and 60, whereas the alloy with $x = 18$ exhibits a more disordered structure of the nanocrystals.

Acknowledgments

This work was supported by the Spanish Government and EU FEDER (project MAT 2001-3175) and by the PAI of the Junta de Andalucía. JSB acknowledges a research fellowship of the DGES.

References

[1] Yoshizawa Y, Oguma S and Yamauchi K 1988 *J. Appl. Phys.* **64** 6044
[2] Suzuki K, Kataoka N, Inoue A, Makino A and Masumoto T 1990 *Mater. Trans. JIM* **31** 743
[3] Suzuki K, Makino A, Kataoka N, Inoue A and Masumoto T 1991 *Mater. Trans. JIM* **32** 93
[4] McHenry M E, Willard M A and Laughlin D E 1999 *Prog. Mater. Sci.* **44** 291
[5] Hernando A, Marín P, Vázquez M, Barandiarán J M and Herzer G 1998 *Phys. Rev.* B **58** 366
[6] Willard M A, Laughlin D E, McHenry M E, Thoma D, Sickafus K, Cross J O and Harris V G 1998 *J. Appl. Phys.* **84** 6773
[7] Müller M, Mattern N and Illgen L 1992 *J. Magn. Magn. Mater.* **112** 263
[8] Bardos D I 1969 *J. Appl. Phys.* **40** 1371
[9] Kulkova S E, Valujsky D V, Kim J S, Lee G and Koo Y M 2002 *Physica* B **322** 236
[10] Jay J Ph, Wojcik M and Panissod P 1996 *Z. Phys.* B **101** 471
[11] DeMayo B, Forester D W and Spooner S 1970 *J. Appl. Phys.* **41** 1319
[12] Vincze I, Campbell I A and Meyer A J 1974 *Solid State Commun.* **15** 1495
[13] Hamdeh H H, Okamoto J and Fultz B 1990 *Phys. Rev.* B **42** 6694
[14] Blázquez J S, Conde A and Grenèche J M 2002 *Appl. Phys. Lett.* **81** 1612
[15] Blázquez J S, Conde C F and Conde A 2001 *J. Non-Cryst. Solids* **287** 187
[16] Blázquez J S, Franco V, Conde C F and Conde A 2003 *J. Magn. Magn. Mater.* **254/255** 460
[17] Blázquez J S, Franco V and Conde A 2002 *J. Phys.: Condens. Matter* **14** 11717
[18] Teillet J and Varret F *MOSFIT Program (Université du Maine, Le Mans)* unpublished
[19] Zhang Y, Blázquez J S, Conde A, Warren P J and Cerezo A 2003 *Mater. Sci. Eng.* A **353** 158
[20] Varret F, Greneche J M and Teillet J 1983 *Proc. Int. Workshop Mössbauer Spectroscopy (Seeheim, 1983)* p 101
[21] Kubaschewski O 1982 Fe–Co, iron–cobalt *Iron—Binary Phase Diagrams* (Berlin: Springer) pp 27–31
[22] Blázquez J S, Lozano-Perez S and Conde A 2002 *Phil. Mag. Lett.* **82** 409